160 km all-optical OFDM transmission system with inline chromatic dispersion compensation

Xingyao Gu (谷星瑶), Hongwei Chen (陈宏伟)*, Minghua Chen (陈明华), and Shizhong Xie (谢世钟)

Tsinghua National Laboratory for Information Science and Technology, Department of Electronic Engineering, Tsinghua University, Beijing 100084, China

**Corresponding author: chenhw@tsinghua.edu.cn*

Received April 18, 2011; accepted June 22, 2011; posted online August 30, 2011

An experimental demonstration of an all-optical sampling orthogonal frequency division multiplexing (AOS-OFDM) transmission system with inline chromatic dispersion (CD) compensation is carried out to test the nonlinear influence. With five subcarriers non-return-to-zero (NRZ) modulated, the total bit rate is 50 Gb/s without polarization multiplexing. The receiver end is highly simplified with direct detection using optical Fourier transform filter. After transmission in 160-km standard single-mode fiber (SSMF) link with 130-ps/nm residual CD, an optimum input optical power for the system performance is achieved.

OCIS codes: 060.4510, 060.4230, 060.3735, 060.4370.
doi: 10.3788/COL201210.020601.

Optical orthogonal frequency division multiplexing (O-OFDM) method has recently drawn increasing attention as a promising technology for future high-speed optical communication systems[1,2]. O-OFDM has high tolerance to chromatic dispersion (CD), polarization mode dispersion, and optical nonlinearity[3−5]. Although it has the above advantages, the high peak-to-average power ratio (PAPR) of O-OFDM, which increases with the number of subcarriers, still limits OFDM system performance because of the nonlinearity. Since the periodic inline CD map is widely used in existing 10-Gb/s transmission systems, the nonlinearity influence on coherent optical OFDM (CO-OFDM) systems is investigated through simulation and experiment[6,7]. The optimum launch power is only –4 dBm because the nonlinearity in a dispersion compensation fiber (DCF) is higher than in a single-mode fiber (SMF). At present, several all-optical OFDM systems were proposed to overcome the electrical bottleneck in CO-OFDM systems[8]. One system was configured using optical inverse discrete Fourier transformers (OIDFTs) based on phase modulators and optical delay lines[9], making the system large and complicated. To make an all-optical OFDM system compact and cost-effective, a system using silica planar lightwave circuit (PLC) fast Fourier transformers (FFTs) based on coupler interferometry[10] was proposed. In Ref. [11], a simple all-optical implementation of a FFT algorithm performing simultaneous serial-to-parallel conversion and FFT calculation within a cascade of delay interferometers (DIs) was introduced. The algorithm requires only passive DIs and scales well with the bit rates. To our knowledge, no direct detection of an all-optical OFDM system with an inline CD map transmission has been reported.

An all-optical sampling (AOS)-OFDM system with optical cyclic postfixes (CPs) inserted was proposed based on a fiber Bragg grating (FBG)[12]. This AOS-OFDM scheme could have better fiber nonlinear tolerance for the low PAPR because of its fewer subcarriers. To obtain better system performance with the same received optical power, the phase pre-emphasis technique in a 50-Gb/s non-return-to-zero (NRZ)-AOS-OFDM system was proposed[13]. In this letter, we conducted an experimental demonstration on the influence of a dispersion map on the 50-Gb/s NRZ-AOS-OFDM system. Each channel has an optimum input optical power for the highest Q factor because of the combined effects of optical signal-to-noise ratio (OSNR) of OFDM signals and fiber nonlinearity.

Similar to the PAPR definition in an electrical domain, the optical PAPR (OPAPR) of O-OFDM signals can be expressed as

$$P_{\mathrm{OPAPR}} = 10\lg\left[\frac{\max(|S(t)|^2)}{E\left(|S(t)|^2\right)}\right] \leqslant 10\lg N, \qquad (1)$$

where $S(t)$ is the signal after the corresponding ODFT in an AOS-OFDM system, $\max(|S(t)|^2)$ is the maximum optical power, $E(|S(t)|^2)$ is the average optical power, and N is the number of subcarriers. It can be seen that OPAPR will increase with the number of subcarriers, which is the same as in the electrical domain. For example, the maximum value in the 256-single carries (SC) OFDM system is 10 lg256 = 24 dB, whereas the one in the 5-SC OFDM system is only 10 lg5 = 7 dB. Thus, because of the less number of subcarriers in the all-optical OFDM system, the OPAPR can be quite lower than that in the CO-OFDM system. To test the OPAPR influence on system performance, an all-optical OFDM transmission system is built as shown in Fig. 1.

An ultra-short optical pulse train with a pulse width of about 2 ps is generated by a mode-locked fiber laser (MLFL) with a repetition rate of 10 GHz. The pulse train from the pulse pattern generator (PPG) is a 2^7–1 pseudo-random bit sequence (PRBS) at 10 Gb/s. Before the signal is modulated with a Mach–Zehnder modulator (MZM), it is fed into an electrical delay line (EDL) which is used to confirm the synchronous unipolar NRZ modulation. Then, the 50-Gb/s NRZ-AOS-OFDM signal is reflected by the multiplexer (MUX) FBG and boosted into a transmission link. At the receiver, a demultiplexer (DMUX) FBG is used as a matched filter by performing

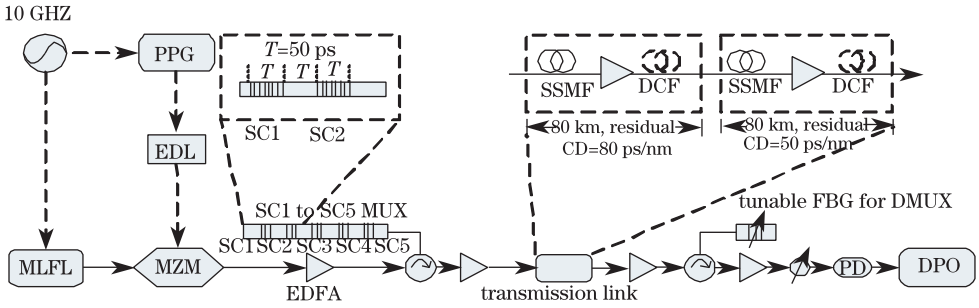

Fig. 1. Experimental setup of the 50-Gb/s NRZ-AOS-OFDM system.

Table 1. Parameters for AOS-OFDM MUX

Channels	MUX			
	M	ΔL (μm)	$\Delta\varphi$	φ_0
SC1	20	512.25	$-n\pi/4$	0
SC2	20	512.25	$-n\pi/8$	π
SC3	20	512.25	0	0
SC4	20	512.25	$n\pi/8$	π
SC5	20	512.25	$n\pi/4$	0

M is the number of sub-gratings in one MUX sub-FBG module; ΔL is the distance between each sub-grating, which equals $cT/n_{\rm eff}M$, where c is the speed of light in a vacuum, $T = 50$ ps is half of the symbol period, and $n_{\rm eff} = 1.464$ is the effective refractive index of the fiber core; $\Delta\varphi$ is the phase shift among the sub-gratings of each channel; φ_0 is the initiation phase of each MUX sub-FBG. With the optimum phase design, the system performance will be improved with the same received optical power[14].

optical Fourier transform[11] to demultiplex corresponding SC channels. The signals after DMUX are amplified and detected with a traditional 10-GHz photon detector (PD). At the receiver end is a digital phosphor oscilloscope (DPO) to save signals for analysis.

In this experiment, five MUX sub-FBGs for each SC channel are made in one FBG whose structure is shown in Fig. 1. The single-way time interval between each sub-FBG is set to 50 ps, which is indicated as T in Fig. 1. To keep five channels synchronous, T equals half of the OFDM symbol period (100 ps). The MUX sub-FBG for the ith subcarrier is designed to have 20 reflection sub-gratings, four of which are CPs. The time delay and phase shift of the nth sub-grating are $(n-1)\times 5/2$ ps and $(i-3)\times(n-1)\,\pi/4$, respectively. The detailed structure parameters of AOS-OFDM MUX are shown in Table 1. The DMUX FBG is designed to have 16 reflection sub-gratings. The time delay between each sub-grating is 2.5 ps, and the phase shift is set to zero. The central frequency of DMUX FBG can be adjusted by stretching to demultiplex corresponding SC channels.

A dispersion map is used in transmission link with two spans. In each span, after 80-km standard SMF (SSMF) whose total cumulated dispersion is 1 394 ps/nm, a DCF is used to compensate for the CD. In the first span, the total dispersion of DCF is –1 314 ps/nm, and in the second one, the total dispersion of DCF is –1 345 ps/nm. The nonlinearity coefficient (γ) of DCF and SSMF is 12 and 1.3 $\rm W^{-1}\ km^{-1}$, respectively. An Er-doped fiber amplifier (EDFA) is used in the middle of SSMF and DCF to compensate for the fiber loss. The gain of EDFA is 25 dB, which can totally compensate for the fiber loss of SSMF and DCF.

In the simulation, the residual CD is set to 0, 30, and 140 ps/nm, respectively, to form different dispersion maps and simulate the Q factor as a function of input optical power for the 50-Gb/s NRZ-AOS-OFDM system. When the residual CD is 0 ps/nm, the system performance is only connected with OSNR and fiber nonlinearity. At low input power, the system degradation is mainly due to the OSNR of O-OFDM signals. Therefore, at the lower input optical powers, the Q factors increase linearly with the input optical power. However, with the increase of input power, the nonlinearity effect starts to degrade the system performance and the Q factor starts to decrease when the input power exceeds the optimum point. As shown in Fig. 2, the optimal input power of NRZ-AOS-OFDM is around 0 dBm. When the residual CD is 30 or 140 ps/nm, the optimal input optical power of the NRZ-AOS-OFDM remains the same as the 0 residual CD condition. The residual CD does not change the trend of the curves because it only affects the Q factor. Therefore, the maximum Q of 140 residual CD is much more decreased by 8 dB than it of 0 residual CD. However, the optimal input power is not changed.

The optical 50-Gb/s NRZ-AOS-OFDM signal spectra

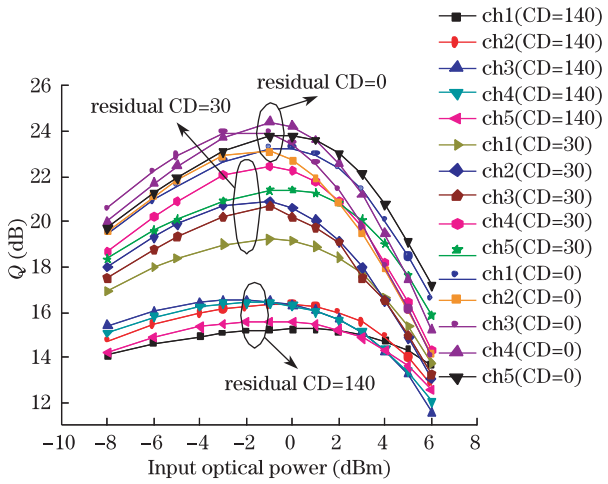

Fig. 2. Q factor as a function of the input optical power for 50-Gb/s NRZ-AOS-OFDM system with different residual CDs.

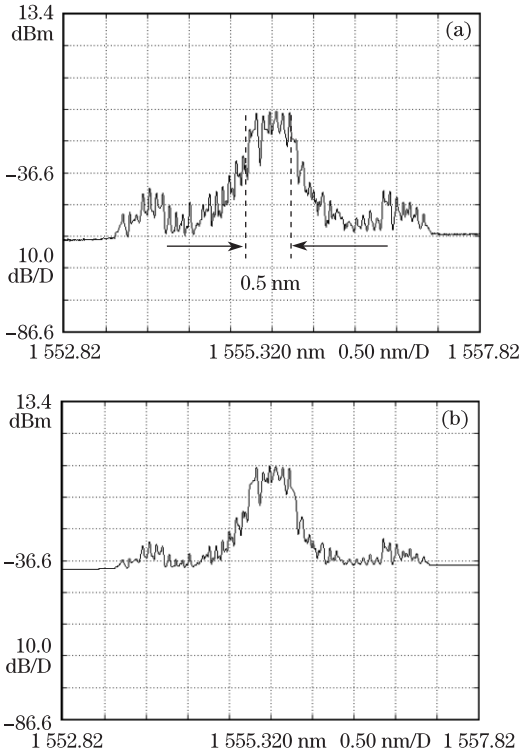

Fig. 3. Optical 50-Gb/s NRZ-AOS-OFDM signal spectra (a) before and (b) after transmission.

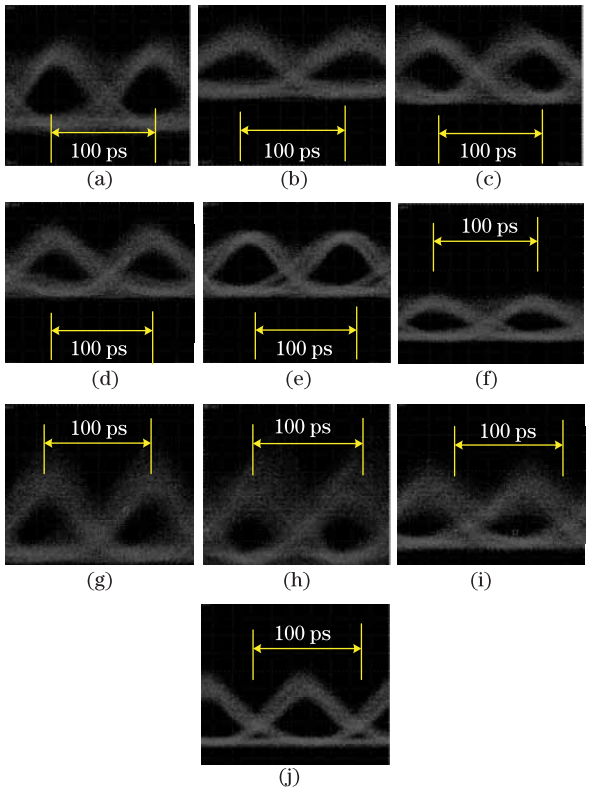

Fig. 4. Demodulated eye diagrams of the first to the fifth subcarrier channel at 0 dBm received optical power for (a)–(e) B2B and (f)–(j) after transmission over two spans.

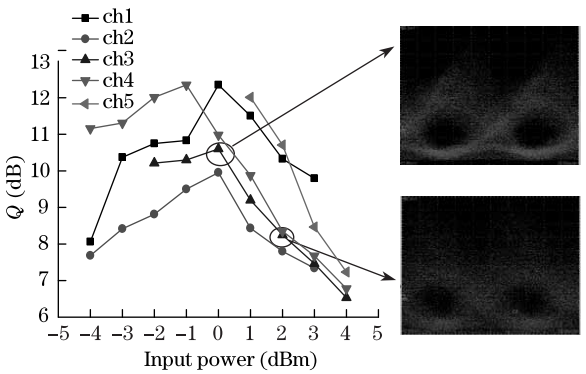

Fig. 5. Q factor as a function of the input optical power for the 50-Gb/s NRZ-AOS-OFDM system after transmission over two spans.

before and after transmission are shown in Fig. 3. The –20-dB bandwidth of the OFDM signal is about 0.5 nm.

Figure 4 shows the eye diagrams of received signals from the first to the fifth subcarriers at 0 dBm received optical power for both back-to-back (B2B) and after transmission over two spans. All the eye diagrams have good opening. The first and fifth subcarriers have better performances than the other three subcarriers because of less cross-disturbance from the neighboring channels.

Figure 5 shows the Q factor as a function of input optical power after transmission over two spans with eye diagrams inserted. Since only collect 10^5 data are collected, the smallest bit error rate (BER) that can be calculated is equal to 10^{-5} and the corresponding max Q factor is 12.4 dB. In Fig. 4, the fifth subcarrier at lower input optical power has larger Q performance than the max Q we can calculate, so it is not shown. From the first to the fourth subcarriers, with input optical power increasing, each channel has an optimum power for the biggest Q factor. The optimal input optical powers of these channels are about 0 dBm. In fact, by optimizing the dispersion map, a bigger optimum input optical power for the max Q factor can be obtained.

In conclusion, the system performance of the 50-Gb/s NRZ-AOS-OFDM system with inline dispersion compensation is shown. The all-optical OFDM signals are successfully transmitted over a 160-km SMF link with direct detection using optical Fourier transform filter. Channels 1–5 are found to have an optimum input optical power of about 0 dBm for the max Q factor because of the combined effects of OSNR of OFDM signals and fiber nonlinearity. In our experiment, there is only one EDFA in each transmission span, which is not optimized. Actually, in a well-designed fiber-optic transmission system, the power into the DCF is controlled so that most of the nonlinear impairments result from the transmission line. Thus, there is still room for all-optical OFDM optimum launched power enhancement compared with CO-OFDM systems.

This work was supported by the National Natural Science Foundation of China (Nos. 60736002, 60807026, 60932004, and 61090391), the Open Fund of Key Laboratory of Optical Communication and Lightwave Technologies (BUPT), Ministry of Education, China, and the State Key Laboratory of Advanced Optical Communication Systems and Networks, China (No. 2008SH03).

References

1. H. C. Bao and W. Shieh, IEEE Photon. Technol. Lett. **19,** 922 (2007).
2. B. J. C. Schmidt, A. J. Lowery, and J. Armstrong, in *Proceedings of OSA/NFOEC 2007* PDP18 (2007).
3. W. Shieh and C. Athaudage, Electron. Lett. **42,** 587 (2006).
4. I. B. Djordjevic, Opt. Express **15,** 3692 (2007).
5. A. J. Lowery, Opt. Express **15,** 12965 (2007).
6. K. Forozesh, S. L. Jansen, S. Randel, I. Morita, and H. Tanaka, in *Proceedings of IEEE/LEOS Summer Topical Meeting* 135 (2008).
7. Y. Tang, Y. Ma, and W. Shieh, in *Proceedings of OSA/OFC/NFOEC 2009* OWW3 (2009).
8. J. Shao, W. Li, and X. Liang, Chin. Opt. Lett. **8,** 875 (2010).
9. K. Lee, C. T. D. Thai, and J. K. Rhee, Opt. Express **16,** 4023 (2008).
10. K. Takiguchi, M. Oguma, T. Shibata, and H. Takahashi, in *Proceedings of OSA/OFC/NFOEC 2009* OWO3 (2009).
11. D. Hillerkuss, A. Marculescu, J. Li, M. Teschke, G. Sigurdsson, K. Worms, S. B. Ezra, N. Narkiss, W. Freude, and J. Leuthold, in *Proceedings of OSA/OFC/NFOEC 2010* OWW3 (2010).
12. H. Chen, M. Chen, and S. Xie, J. Lightwave Technol. **27,** 4848 (2009).
13. H. Chen, C. Tang, F. Yin, M. Chen, and S. Xie, Chin. Opt. Lett. **8,** 871 (2010).
14. C. Tang, H. Chen, F. Yin, M. Chen, and S. Xie, in *Proceedings of OSA/OFC/NFOEC 2010* OWO5 (2010).